PHYSICAL REVIEW B **91**, 235116 (2015)

Bulk electronic structure of Zn-Mg-Y and Zn-Mg-Dy icosahedral quasicrystals

J. Nayak,[1] M. Maniraj,[1] A. Gloskovskii,[2] M. Krajčí,[3] S. Sebastian,[4] I. R. Fisher,[4] K. Horn,[5] and S. R. Barman[1,*]
[1]*UGC-DAE Consortium for Scientific Research, Khandwa Road, Indore, 452001, Madhya Pradesh, India*
[2]*Deutsches Elektronen-Synchrotron DESY, Notkestr. 85, D-22607 Hamburg, Germany*
[3]*Institute of Physics, Slovak Academy of Sciences, Dúbravská cesta 9, SK-84511 Bratislava, Slovak Republic*
[4]*Geballe Laboratory for Advanced Materials and Department of Applied Physics, Stanford University, California 94305-4045, USA*
[5]*Fritz-Haber-Institut der Max-Planck-Gesellschaft, Faradayweg 4-6, D-14195 Berlin, Germany*
(Received 21 March 2015; revised manuscript received 19 May 2015; published 11 June 2015)

We use bulk sensitive hard x-ray photoelectron spectroscopy to provide unambiguous evidence for a pseudogap in the density of states around the Fermi level in icosahedral Zn-Mg-Y and Zn-Mg-Dy quasicrystals, in agreement with our density functional theory calculations. The pseudogap in these Zn-based quasicrystals is less pronounced compared to the Al-based ones such as Al-Pd-Mn and Al-Cu-Fe [J. Nayak *et al.*, Phys. Rev. Lett. **109**, 216403 (2012)]. This observation is in agreement with transport studies that indicate a larger charge carrier concentration in the Zn-based quasicrystals. Compared to Zn-Mg-Dy, the pseudogap is somewhat deeper in Zn-Mg-Y. The larger width of the Mg 1s and Zn 2p core-level spectra in Zn-Mg-Y is explained by different configurations of the local atomic surrounding compared to Zn-Mg-Dy.

DOI: 10.1103/PhysRevB.91.235116 PACS number(s): 71.23.Ft, 79.60.−i

I. INTRODUCTION

The discovery of thermodynamically stable icosahedral Zn-based quasicrystals (QC) [1] ushered in an intensive research on their structural, transport, and electronic properties [2–5]. There is a growing body of theoretical and experimental evidence that the fundamental reason for the formation of quasicrystalline order is the presence of a pseudogap around the Fermi level [6–10].

However, the electronic contribution to the specific heat in Zn-Mg-Y was reported to be similar to Zn metal, indicating no reduction of the density of states (DOS) at E_F [4], although in the same work a distinct feature that was assigned to an excitation across a pseudogap was observed from an optical conductivity study [4]. It was also reported [11] that their resistivity (150–200 $\mu\Omega$ cm) is an order of magnitude lower than Al-based quasicrystals such as Al-Pd-Mn [12] or highly conducting compositions of Al-Pd-Re [13], again pointing towards a higher DOS at E_F in the former. Since photoelectron spectroscopy is a direct probe of the electron states, the pseudogap has been studied extensively using this technique, albeit with low photon energies (ultraviolet to soft x-ray range) that provided information about the *surface* electronic structure because of the small escape depth of photoelectrons with low kinetic energy [2,5,14,15]. This surface sensitivity may give rise to erroneous conclusions because the surface structure may deviate from that of the bulk, giving rise to a change in electronic structure. This may well be the reason why in these studies, a pseudogap was not observed in icosahedral (i)-Zn-Mg-Y by Stadnik *et al.* [2]; rather a clear existence of a metallic Fermi edge was established, with a linearly decreasing intensity from higher binding energies towards E_F. Suchodolskis *et al.* [5], working on single grain i-Zn-Mg-Y, also observed a metallic Fermi edge. On the other hand, the DOS calculations using density functional theory for a hexagonal approximant to Zn-Mg-Y showed the existence of a pronounced pseudogap around the Fermi level, due to a strong hybridization between the s and p-d states related to Y [16,17].

Here, we report a photoemission spectroscopy study of icosahedral Zn-Mg-Y and Zn-Mg-Dy quasicrystals using hard x-ray photons that probe the true *bulk* electronic structure with a sampling depth extending into the range of ≈120 Å. The results are compared with *ab initio* theoretical calculations. We unambiguously establish the existence of a pseudogap, although not as pronounced as Al-based quasicrystals such as Al-Pd-Mn or Al-Cu-Fe [10]. The present work resolves the continuing disagreement between *ab initio* density functional theory and the results from surface sensitive photoemission spectroscopy [2,5].

II. EXPERIMENTAL AND CALCULATIONAL DETAILS

Single grain icosahedral $Zn_{57}Mg_{34}Y_9$ and $Zn_{57}Mg_{34}Dy_9$ quasicrystals were grown by slow cooling a ternary melt, as discussed in Ref. [18]. Hard x-ray photoelectron spectroscopy measurements were performed at the P09 beamline [19] at Petra III, Deutsches Elektronen-Synchrotron, Hamburg using a Si(111) double crystal monochromator. All measurements were performed with 7.93-keV photon energy at 40 K. Although post-monochromators reduce the intensity of the photon beam, a Si(333) post-monochromator was used to improve the energy resolution and stability. The spectra were recorded with a Phoibos 225 HV electron energy analyzer from Specs Surface Nano Analysis GmbH, Germany with base pressure of 4×10^{-10} mbar in the analysis chamber. In order to obtain a contamination free surface, the samples were scraped *in situ* by diamond file in a vacuum of 4×10^{-9} mbar. In order to maximize the bulk sensitivity and optimize the signal to background ratio, linearly polarized x rays were incident at almost grazing angle (5° with the surface) and the electrons were detected in nearly normal emission geometry with the E field vector and the dipole cone pointing into the direction of the analyzer. The overall resolution (300 meV) including both the source and the analyzer contributions was obtained by fitting the Fermi edge spectrum of Au that was in

---

[*] barmansr@gmail.com

1098-0121/2015/91(23)/235116(6)

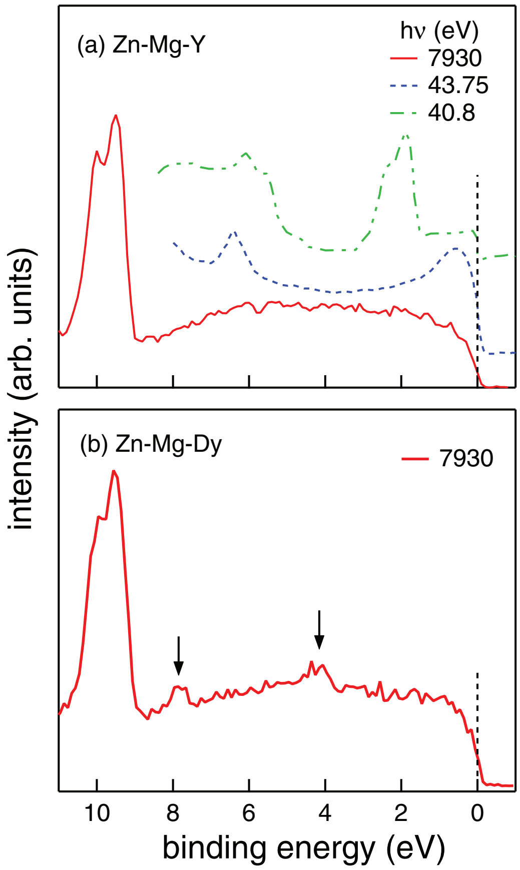

FIG. 1. (Color online) (a) HAXPES valence band spectrum of Zn-Mg-Y recorded with 7.93-keV photon energy at 40 K compared with surface sensitive low energy photoemission spectra published by Stadnik *et al.* [2] (green dot-dashed line) and by Suchodolskis *et al.* [5] (blue dashed line). (b) HAXPES valence band spectrum of Zn-Mg-Dy recorded at 40 K.

electrical contact with the specimen. A nonlinear least square curve fitting was performed using the Levenberg-Marquardt algorithm, as in our earlier work [20].

Density functional theoretical (DFT) calculations have been performed by using the VASP code [21] considering 1/1 approximant (which has a local structure that is very similar to quasicrystals but is periodic with a large unit cell) consisting of 160 atoms in a cubic cell (96 Zn, 50 Mg, and 14 Y/Dy atoms) [22]. The valence $4f$ states of Dy are shifted to the core states because of the problem of DFT with the correct description of f electrons.

III. RESULTS AND DISCUSSION

The HAXPES valence band spectra of Zn-Mg-Y is shown in Fig. 1(a) and compared with the low energy photoemission data reported by Stadnik *et al.* [2] and Suchodolskis *et al.* [5]. The spectrum shows the Zn $3d_{5/2}$ and $3d_{3/2}$ spin-orbit split peaks at 9.5 and 10 eV, in good agreement with the low energy photoemission data [2,5]. The UPS spectrum from Stadnik *et al.* shows a feature around 6 eV; this peak is absent in the HAXPES spectrum. Another doublet peak around 2 eV has been ascribed to the Zn $3d$ peak excited by the He II* satellite line at 48.4-eV photon energy [2]. The shape of the spectrum near E_F that has been recorded with 43.75-eV photon energy by Suchodolskis *et al.* [5] for single grain Zn-Mg-Y specimens cleaved *in situ* shows a peak centered at 0.7 eV that was attributed to a pseudogap structure related to a van Hove singularity [5]. However, this interpretation was neither reported by Stadnik *et al.* [2] nor derived from density functional theory [16,17].

In contrast to the conflicting results from low energy photoemission valence band spectra published in literature, the bulk electronic structure of Zn-Mg-Y has been recorded with a probing depth of ≈120 Å at 7.93 keV that has been calculated using the Tanuma, Powell, and Penn algorithm [23,24]. The HAXPES valence band spectrum exhibits a featureless convex rounded shape from the lower binding energy side of the Zn $3d$ peak up to the Fermi level [Fig. 1(a)]. The HAXPES valence band spectrum of Zn-Mg-Dy [Fig. 1(b)] exhibits the Zn $3d$ spin-orbit split peaks at similar binding energies as Zn-Mg-Y. However, in contrast to Zn-Mg-Y, here two distinct peaks are observed at 4 eV and 8 eV [black arrows in Fig. 1(b)]. Their origin can be traced to the fact that Dy is a rare earth f element with $4f^{10}6s^2$ configuration. The experimental XPS valence band of Dy metal exhibits multiplet structures related to the localized $4f$ level around 4 and 8 eV [25], and hence the peaks in the Zn-Mg-Dy valence band in Fig. 1(b) can be attributed to Dy $4f$ states. Similar multiplet features originating from Ho $4f$ states have been observed at about 6 eV in Zn-Mg-Ho [26]. Such features are absent in Zn-Mg-Y [Fig. 1(b)] since Y is a $4d$ metal with $4d^1 5s^2$ configuration.

The HAXPES valence band spectrum of Zn-Mg-Y near E_F is evidently suppressed compared to the low energy surface sensitive spectra, as seen in the close-up spectra in Fig. 2(a). From Fig. 2(b), where all the spectra have been normalized to the same intensity around 1.5 eV binding energy, it is clear that Zn-Mg-Y has a markedly lower intensity compared to Zn-Mg-Dy, indicating the presence of a deeper pseudogap in the former. Interestingly, Zn-Mg-Dy exhibits a higher contribution of spectral intensity compared to Al-Cu-Fe, as well as Al-Pd-Mn [Fig. 2(b)], indicating that the pseudogap is least pronounced in Zn-Mg-Dy. This is confirmed by the quantitative extraction of the pseudogap using least square fitting discussed below. In order to emulate the shape of the pseudogap using least squares fitting, we use the following model function:

$$[I \times S(E) \times f(E,E_F)] \otimes G(E,\sigma), \tag{1}$$

where $S(E)$ is the spectral function that represents the shape of the pseudogap, an inverted Lorentzian function [2,10,27] centered at E_F,

$$S(E) = (aE + b) \times \left(1 - \frac{C_L \Gamma_L^2}{E^2 + \Gamma_L^2}\right), \tag{2}$$

where $2\Gamma_L$ is the full width at half maximum of the Lorentzian function and C_L is the depth of the pseudogap, a parameter that is allowed to vary between 0 and 1. $C_L = 0$ implies absence of the pseudogap and $S(E)$ is a line defined by $(aE + b)$. $C_L = 1$ implies a fully formed pseudogap with $S(E) = 0$ at $E = 0$, i.e., at E_F. $f(E,E_F)$ is the Fermi function, $G(E,\sigma)$ is the Gaussian representing the instrumental resolution, and I is a multiplicative parameter. The position of E_F and the resolution

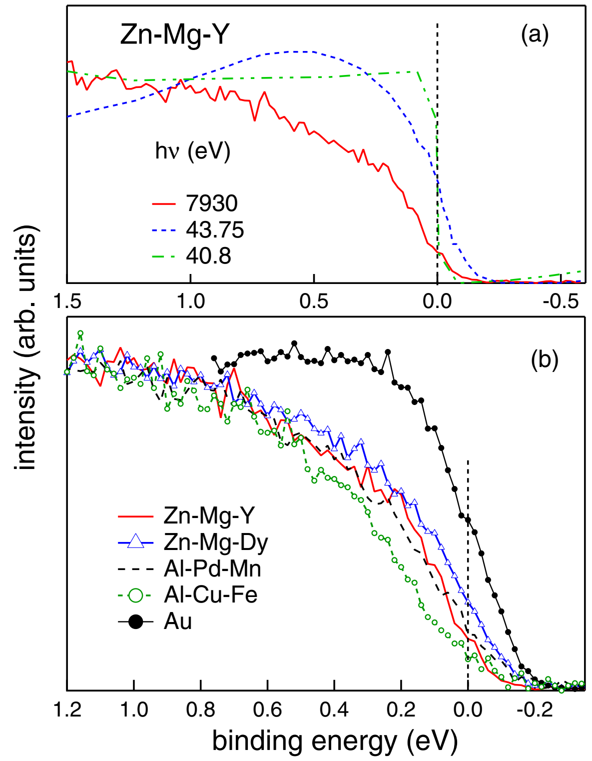

FIG. 2. (Color online) The near E_F HAXPES valence band spectrum of (a) Zn-Mg-Y compared with low energy photoemission spectra from Stadnik *et al.* [2] (green dot-dashed line, energy resolution 30 meV) and from Suchodolskis *et al.* [5] (blue dashed line, energy resolution 230 meV). (b) HAXPES valence band spectrum of Zn-Mg-Y compared with Zn-Mg-Dy. The Au Fermi edge, Al-Cu-Fe, and Al-Pd-Mn spectra from Nayak *et al.* [10] are also shown for comparison.

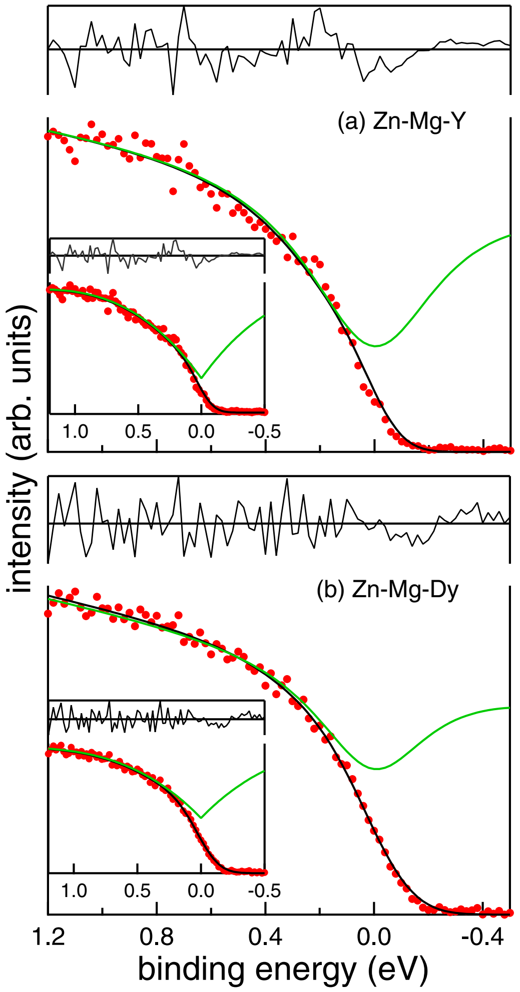

FIG. 3. (Color online) HAXPES valence band spectra (red solid circles) of (a) Zn-Mg-Dy and (b) Zn-Mg-Y in the near-E_F region. The experimental valence band spectra, fitted with an inverted Lorentzian function [$S(E)$, green line] show a pseudogap at E_F. The resulting fitted curve is shown as a black line. The residuals are shown at the top of each panel. Insets show the least square curve fitting using a third-order polynomial function.

were determined by fitting of the Au Fermi edge spectrum by the Fermi function multiplied by a constant DOS. The E_F position and the resolution were kept fixed during the fitting.

The presence of a pseudogap (shown by solid green line) is unambiguously observed for both Zn-Mg-Y ($C_L = 0.6$) and Zn-Mg-Dy ($C_L = 0.45$) in Fig. 3. The quality of the fit is very good, as shown by the residuals. Compared to the Al-based quasicrystals (such as Al-Pd-Mn with $C_L = 0.72$ and Al-Cu-Fe with $C_L = 1$), Zn-based quasicrystals exhibit a shallower pseudogap. This important observation is consistent with transport measurements [11], which suggest an enhanced charge carrier density in rare-earth-based quasicrystals compared to the conventional ones. Moreover, the Zn-based quasicrystals not only exhibit a shallower pseudogap, but also a larger full width at half maximum, $2\Gamma_L$ (Table I) compared to Al-based quasicrystals (0.37 eV) [10]. The observation of a pseudogap in Zn-Mg-Y is supported by the optical conductivity spectrum that exhibits a clear feature characteristic of excitations across a pseudogap [4]. Moreover, the significantly low carrier concentration obtained from the Hall measurement is in accordance with the presence of a pseudogap [4]. On the other hand, a relatively large value of the electronic part of the specific heat of Zn-Mg-Y reported in Ref. [4] might be related to the contribution of the tunneling states [28] to the specific heat of icosahedral quasicrystals.

TABLE I. Parameters obtained from the least square curve fitting of the near E_F spectra recorded with 7.93 keV at 40 K using different model functions.

Specimen	Model function	Parameter values
Zn-Mg-Y	Lorentzian	$C_L = 0.6 \pm 0.02$, $2\Gamma_L = 0.6 \pm 0.04$
	Third-order polynomial	$A_P = 1.5 \pm 0.15$, $B_P = -1 \pm 0.3$, $C_P = 0.2 \pm 0.15$, and $D_P = 0.3 \pm 0.03$
Zn-Mg-Dy	Lorentzian	$C_L = 0.45 \pm 0.02$, $2\Gamma_L = 0.5 \pm 0.04$
	Third-order polynomial	$A_P = 1.2 \pm 0.15$, $B_P = -0.8 \pm 0.25$, and $C_P = 0.15 \pm 0.1$, $D_P = 0.5 \pm 0.02$

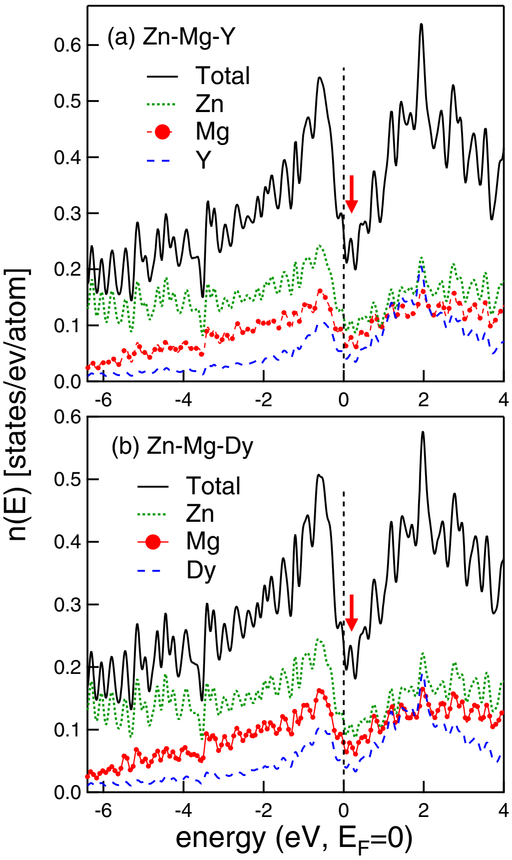

FIG. 4. (Color online) The total DOS and the partial DOS of (a) Zn-Mg-Y and (b) Zn-Mg-Dy calculated by density functional theory using the VASP code.

In order to establish that the parameter values are independent of the model function, we have used another fitting function, a third-order polynomial [10]:

$$S(E) = D_P + A_P|E| + B_P|E|^2 + C_P|E|^3, \qquad (3)$$

where A_P, B_P, and C_P are the coefficients that define its shape, while $D_P = 0$ would imply zero DOS at E_F. From the least square curve fitting in the same range (inset of Fig. 3), it is clear that the fitting is equally good: $\chi^2 = 0.027$ (0.027) for the third-order polynomial function whereas $\chi^2 = 0.029$ (0.059) for the inverted Lorentzian for Zn-Mg-Dy (Zn-Mg-Y). The parameter related to the depth of the pseudogap D_P is 0.5 for Zn-Mg-Dy (see Table I). The depth of the pseudogap for Zn-Mg-Y is 0.3. Thus, the depth of the pseudogap is smaller in Zn-Mg-Dy compared to Zn-Mg-Y. This is in agreement with the result obtained using the inverted Lorenzian function [Fig. 2(c)]. This establishes that the relative variation of the most important quantitative parameter, i.e., the depth of the pseudogap (Fig. 3) between the two quasicrystals is independent of the model function used.

The density of states of both Zn-Mg-Y and Zn-Mg-Dy calculated here by density functional theory exhibits a featureless shape and the presence of a distinct pseudogap around E_F (Fig. 4), in good agreement with the HAXPES spectra (Figs. 1–3). However, the two peaks at 4 and 8 eV in the valence band spectrum of Zn-Mg-Dy [Fig. 1(b)] are not observed in Fig. 4(b) since the $4f$ states have been shifted from the valence band to the core states. It may be noted that the noisy or spiky character of DOS originates from the almost dispersionless energy bands of quasicrystalline approximants. The similarity in the shape of the Zn, Mg as well as the Y/Dy partial DOS indicates a strong hybridization between the s, p, and d states. Interestingly, the minimum of the pseudogap derived from theory is 0.2 eV above E_F, as shown by the red arrows in Fig. 4, and this is observed from the partial DOS also. The width of the pseudogap from theory is more than 1 eV, which is larger than what we obtain from HAXPES (0.5–0.6 eV). However, this finds a straightforward explanation by the fact that in HAXPES we only observe the occupied part of the pseudogap below E_F, and assume it to be symmetrical below and above E_F. The theoretical DOS, on the other hand, shows that it widens asymmetrically above E_F. A similar behavior of the pseudogap has been observed in the calculated DOS of Al-Pd-Mn [29].

The core-level spectra recorded with hard x rays reveal interesting characteristics of the electronic structure of these quasicrystals. The spectra often exhibit loss peaks at higher binding energies with respect to the main peak originating from collective plasmon excitations. The behavior of these loss peaks can provide important information about hybridization between the different electron states. Besides, the shape and position of the core-level main peak can be used to identify the electronic excitations and depict the influence of the local chemical surrounding.

The main peak of the Mg $1s$ HAXPES core-level spectrum appears at 1303.6-eV binding energy for both Zn-Mg-Y and Zn-Mg-Dy [Fig. 5(a)]. It shows an extra feature (indicated by an arrow) at about 12 eV ($=\omega_p$) from the main peak for both Zn-Mg-Y and Zn-Mg-Dy, which we assign to a bulk plasmon loss; no surface plasmon losses are observed. This value is somewhat larger than Mg metal ($\omega_p = 10.6$ eV) [30] possibly due to hybridization of the Mg s, p with the Zn d bands. The binding energy of the Zn $2p_{3/2}$ (1021.6 eV) and $2p_{1/2}$ (1044.5 eV) peaks is similar between the two quasicrystals [Fig. 5(b)]. Although in the late $3d$ transition metals, the plasmon loss features are weak and shifted to higher energies [31], bulk plasmon peaks are clearly observed at the same loss energy as in Mg $1s$ (12 eV) for both the spin-orbit split Zn $2p$ peaks. In Al-Mn alloys, the appearance of Al-related bulk plasmons has been reported in Mn $2p$ core-level spectra due to hybridization of Al s, p, and Mn d states [32]. In this case also, hybridization between Mg s, p, and Zn d states leads to the appearance of Mg-related bulk plasmon in the Zn $2p$ spectrum.

An interesting difference between the core-level spectra of Zn-Mg-Y and Zn-Mg-Dy is the larger width in the former. This is evident from the insets of Fig. 5 for both Mg $1s$ and Zn $2p$. The full width at half maximum (FWHM) for Zn-Mg-Y (Zn-Mg-Dy) is 1 eV (0.75 eV) for Zn $2p_{3/2}$. The FWHM of the Mg $1s$ line is 1 and 0.7 eV for Zn-Mg-Y and Zn-Mg-Dy, respectively. The larger width of Mg $2p$ core-level spectra in Zn-Mg-Y with respect to the crystalline Zn_2Mg Laves phases was related to different local surroundings, i.e., the number of inequivalent sites of the Mg atoms that induce different shifts resulting in a broadened spectrum [33]. It can be thus concluded that the reduced FWHM in Zn-Mg-Dy indicates the presence of a smaller number of Mg and Zn inequivalent sites compared to Zn-Mg-Y. This points to a difference in the structure of icosahedral Zn-Mg-Dy and Zn-Mg-Y.

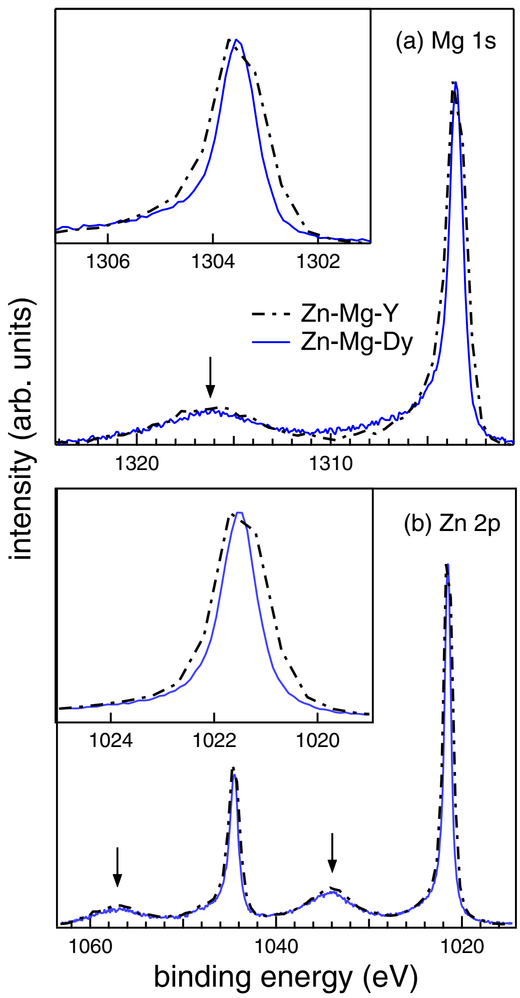

FIG. 5. (Color online) (a) Mg 1s and (b) Zn 2p core-level spectra of Zn-Mg-Y and Zn-Mg-Dy, with the main peak normalized to same intensity. The inset shows the main peak in an expanded scale.

IV. CONCLUSION

Hard x-ray photoelectron spectroscopy has been employed to unravel the bulk electronic structure of Zn-based icosahedral quasicrystals such as Zn-Mg-Y and Zn-Mg-Dy. We provide clear evidence for a pseudogap at E_F for both materials from a least square fitting of the spectral shape near E_F. Density functional theory also unambiguously shows the presence of a pseudogap that widens asymmetrically above E_F. We find that the pseudogap in Zn-based quasicrystals is shallower compared to Al-based quasicrystals such as Al-Pd-Mn and Al-Cu-Fe, in agreement with their transport properties. The shape of the HAXPES valence band in Zn-Mg-Y and Zn-Mg-Dy is markedly different from that studied so far by low energy photoemission [2,5]. This may be related to the intrinsic difference between the surface and the bulk electronic structure, or artifacts in the low energy photoemission data. In the core-level spectra of both Mg 1s and Zn 2p, the bulk plasmon peak is observed at about 12 eV loss energy. The larger width of both Mg 1s and Zn 2p core-level spectra in Zn-Mg-Y compared to the Zn-Mg-Dy indicates a smaller number of inequivalent sites in the latter.

ACKNOWLEDGMENTS

The India-Germany Collaborative project funded by the Department of Science and Technology is thankfully acknowledged. Funding for the HAXPES instrument at beamline P09 by the Federal Ministry of Education and Research (BMBF) under Contracts No. 05KS7UM1, No. 05K10UMA, No. 05KS7WW3, No. 05K10WW1, and No. 05K13WW1 is gratefully acknowledged. R. Claessen (University of Würzburg), C. Felser (University of Mainz), and DESY are thanked for providing the HAXPES end station. F. Okrent is thanked for skillful support. We would like to thank J. Zegenhagen, W. Drube, D. D. Sarma, and M. K. Sanyal for support and encouragement. J.N. and M.M. thank Council for Scientific and Industrial Research, India for research fellowships. M.K. thanks the Grant Agency VEGA (Grant No. 2/0189/14) for support. The work at Stanford University is supported by NSF Grant No. DMR-0134613.

---

[1] Z. Luo, S. Zhang, Y. Tang, and D. Zhao, Scr. Metall. **28**, 1513 (1993).

[2] Z. M. Stadnik, D. Purdie, M. Garnier, Y. Baer, A.-P. Tsai, A. Inoue, K. Edagawa, S. Takeuchi, and K. H. J. Buschow, Phys. Rev. B **55**, 10938 (1997).

[3] E. Abe and A. P. Tsai, Phys. Rev. Lett. **83**, 753 (1999); E. Abe, T. J. Sato, and A. P. Tsai, *ibid.* **82**, 5269 (1999).

[4] M. A. Chernikov, S. Paschen, E. Felder, P. Vorburger, B. Ruzicka, L. Degiorgi, H. R. Ott, I. R. Fisher, and P. C. Canfield, Phys. Rev. B **62**, 262 (2000).

[5] A. Suchodolskis, W. Assmus, L. Giovanelli, U. O. Karlsson, V. Karpus, G. Le Lay, R. Sterzel, and E. Uhrig, Phys. Rev. B **68**, 054207 (2003).

[6] J. Hafner and M. Krajčí, Phys. Rev. Lett. **68**, 2321 (1992).

[7] D. N. Davydov, D. Mayou, C. Berger, C. Gignoux, A. Neumann, A. G. M. Jansen, and P. Wyder, Phys. Rev. Lett. **77**, 3173 (1996).

[8] J.-M. Dubios, *Useful Quasicrystals* (World Scientific, London/ Singapore, 2005).

[9] R. Widmer, P. Gröning, M. Feuerbacher, and O. Gröning, Phys. Rev. B **79**, 104202 (2009).

[10] J. Nayak, M. Maniraj, A. Rai, S. Singh, P. Rajput, A. Gloskovskii, J. Zegenhagen, D. L. Schlagel, T. A. Lograsso, K. Horn, and S. R. Barman, Phys. Rev. Lett. **109**, 216403 (2012).

[11] I. R. Fisher, K. O. Cheon, A. F. Panchula, P. C. Canfield, M. Chernikov, H. R. Ott, and K. Dennis, Phys. Rev. B **59**, 308 (1999).

[12] I. R. Fisher, M. J. Kramer, T. A. Wiener, Z. Islam, A. R. Ross, T. A. Lograsso, A. Kracher, A. I. Goldman, and P. C. Canfield, Phil. Mag. B **79**, 1673 (1999).

[13] I. R. Fisher, X. P. Xie, I. Tudosa, C. W. Gao, C. Song, P. C. Canfield, A. Kracher, K. Dennis, D. Abanoz, and M. J. Kramer, Phil. Mag. B **82**, 1089 (2002).

[14] E. Rotenberg, W. Theis, K. Horn, and P. Gille, Nature (London) **406**, 602 (2000).

[15] G. Neuhold, S. R. Barman, K. Horn, W. Theis, P. Ebert, and K. Urban, Phys. Rev. B **58**, 734 (1998); K. Horn, W. Theis, J. J.

Paggel, S. R. Barman, E. Rotenberg, Ph. Ebert, and K. Urban, J. Phys.: Condens. Matter **18**, 435 (2006).
[16] M. Krajčí and J. Hafner, J. Phys.: Condens. Matter **12**, 5831 (2000).
[17] K. Oshio and Y. Ishii, J. Alloys Compd. **341**, 402 (2002).
[18] I. R. Fisher, Z. Islam, A. F. Panchula, K. O. Cheon, M. J. Kramer, P. C. Canfield, and A. I. Goldman, Phil. Mag. B **77**, 1601 (1998); I. R. Fisher, M. J. Kramer, Z. Islam, T. A. Wiener, A. Kracher, A. R. Ross, T. A. Lograsso, A. I. Goldman, and P. C. Canfield, Mat. Sci. Eng. A **294**, 10 (2000).
[19] J. Strempfer, S. Francoual, D. Reuther, D. K. Shukla, A. Skaugen, H. Schulte-Schrepping, T. Kracht, and H. Franz, J. Synchrotron Rad. **20**, 541 (2013); A. Gloskovskii *et al.*, J. Electron Spectros. Relat. Phenom. **185**, 47 (2012).
[20] C. Biswas, A. K. Shukla, S. Banik, S. R. Barman, and A. Chakrabarti, Phys. Rev. Lett. **92**, 115506 (2004).
[21] G. Kresse and J. Furthmüller, Phys. Rev. B **54**, 11169 (1996); G. Kresse and D. Joubert, *ibid.* **59**, 1758 (1999).
[22] M. Mihalkovič and M. Widom, [http://alloy.phys.cmu.edu/].
[23] S. Tanuma, C. J. Powell, and D. R. Penn, Surf. Interface Anal. **43**, 689 (2011); C. J. Powell, A. Jablonski, I. S. Tilinin, S. Tanuma, and D. R. Penn, J. Electron Spectrosc. Relat. Phenom. **98-99**, 1 (1999).
[24] C. S. Fadley, J. Electron Spectros. Relat. Phenom. **178-179**, 2 (2010).
[25] J. K. Lang, Y. Baer, and P. A. Cox, J. Phys: F Metal Phys. **11**, 121 (1981).
[26] A. Suchodolskis, W. Assmus, L. Giovanelli, U. O. Karlsson, V. Karpus, G. Le Lay, and E. Uhrig, J. Phys. Condens. Matter **16**, 9137 (2004).
[27] M. Mori, S. Matsuo, T. Ishimasa, T. Matsuura, K. Kamiya, H. Inokuchi, and T. Matsukawa, J. Phys. Condens. Matter **3**, 767 (1991).
[28] P. W. Anderson, B. I. Halperin, and C. M. Varma, Philos. Mag. **25**, 1 (1972).
[29] M. Maniraj, A. Rai, S. R. Barman, M. Krajčí, D. L. Schlagel, T. A. Lograsso, and K. Horn, Phys. Rev. B **90**, 115407 (2014).
[30] P. M. Th. M. van Attekum, and J. M. Trooster, Phys. Rev. B **20**, 2335 (1979).
[31] N. Moslemzadeh, G. Beamson, P. Tsakiropoulos, J. F. Watts, S. R. Haines, and P. Weightman, J. Electron Spectros. Relat. Phenom. **152**, 129 (2006); M. Futsuhara, K. Yoshioka, and O. Takai, Thin Solid Films **322**, 224 (1998).
[32] A. K. Shukla, C. Biswas, R. S. Dhaka, S. C. Das, P. Krüger, and S. R. Barman, Phys. Rev. B **77**, 195103 (2008).
[33] V. Karpus, A. Suchodolskis, J. Taulavičius, U. O. Karlsson, G. Le Lay, W. Assmus, and S. Brühne, Phys. Rev. B **76**, 155119 (2007).